Protein Science (1995), *4*:44–57. Cambridge University Press. Printed in the USA.

Crystallographic study of the structure of colipase and of the interaction with pancreatic lipase

MARIE-PIERRE EGLOFF,[1] LOUIS SARDA,[2] ROBERT VERGER,[3] CHRISTIAN CAMBILLAU,[1] AND HERMAN VAN TILBEURGH[1,4]

[1] Laboratoire de Cristallisation et Cristallographie des Macromolécules Biologiques, URA 1296-CNRS, Faculté de Médecine Nord, 13916 Marseille CX20, France
[2] Institut de Chimie Biologique, Faculté des Sciences Saint-Charles, 3 place Victor Hugo, 13331 Marseille, France
[3] Laboratoire de Lipolyse enzymatique, UPR9025 du GDR1000-CNRS, 31 Chemin Joseph Aiguier, 13402 Marseille Cedex 20, France

(RECEIVED July 28, 1994; ACCEPTED October 17, 1994)

Abstract

Colipase (M_r 10 kDa) confers catalytic activity to pancreatic lipase under physiological conditions (high bile salt concentrations). Previously determined 3-Å-resolution X-ray structures of lipase-colipase complexes have shown that, in the absence of substrate, colipase binds to the noncatalytic C-terminal domain of pancreatic lipase (van Tilbeurgh H, Sarda L, Verger R, Cambillau C, 1992, *Nature 359*:159–162; van Tilbeurgh et al., 1993a, *Nature 362*:814–820). Upon lipid binding, conformational changes at the active site of pancreatic lipase bring a surface loop (the lid) in contact with colipase, creating a second binding site for this cofactor. Covalent inhibition of the pancreatic lipase by a phosphonate inhibitor yields better diffracting crystals of the lipase–colipase complex. From the 2.4-Å-resolution structure of this complex, we give an accurate description of the colipase. It confirms the previous proposed disulfide connections (van Tilbeurgh H, Sarda L, Verger R, Cambillau C, 1992, *Nature 359*:159–162; van Tilbeurgh et al., 1993a, *Nature 362*:814–820) that were in disagreement with the biochemical assignment (Chaillan C, Kerfelec B, Foglizzo E, Chapus C, 1992, *Biochem Biophys Res Commun 184*:206–211). Colipase lacks well-defined secondary structure elements. This small protein seems to be stabilized mainly by an extended network of five disulfide bridges that runs throughout the flatly shaped molecule, reticulating its four finger-like loops. The colipase surface can be divided into a rather hydrophilic part, interacting with lipase, and a more hydrophobic part, formed by the tips of the fingers. The interaction between colipase and the C-terminal domain of lipase is stabilized by eight hydrogen bonds and about 80 van der Waals contacts. Upon opening of the lid, three more hydrogen bonds and about 28 van der Waals contacts are added, explaining the higher apparent affinity in the presence of a lipid/water interface. The tips of the fingers are very mobile and constitute the lipid interaction surface. Two detergent molecules that interact with colipase were observed in the crystal, covering part of the hydrophobic surface.

Keywords: colipase; detergent; lipase; protein structure; triglyceride hydrolysis; X-ray crystallography

In mammals, dietary triglycerides are mainly hydrolyzed in the duodenum by the action of pancreatic lipase (EC 3.1.1.3). The hydrolysis products, fatty acids and monoglycerides, can be taken up by the intestinal wall only when presented as mixed micelles with bile salts. These amphipathic molecules remove proteins, including pancreatic lipase, from the lipid/water interface (Desnuelle, 1986), thus preventing the hydrolysis of long-chain triglycerides by this enzyme. In order to display catalytic activity in the presence of bile salts, pancreatic lipase (M_r 50 kDa) needs a small protein, called colipase (M_r 10 kDa), cosecreted by the pancreas. This cofactor anchors pancreatic lipase to the lipid/water interface without affecting its turnover rate.

Colipase is secreted as a proform (procolipase) that is proteolytically cleaved at position five of the N-terminus (Borgström et al., 1979; Erlanson-Albertsson, 1981). Colipase and procolipase are equally capable of activating pancreatic lipase, but some differences have been observed in the hydrolysis kinetics of long-chain triglycerides. The N-terminal peptide of pro-

Reprint requests to: Christian Cambillau, Laboratoire de Cristallisation et Cristallographie des Macromolécules Biologiques, URA 1296-CNRS, Faculté de Médecine Nord, 13916 Marseille CX20, France; e-mail: cambilau@lccmb.cnrs-mrs.fr.

[4] Present address: Centre de Biochimie structurale, CNRS-UMR C9955/INSERM U414, Faculté de Pharmacie, 15 Avenue Charles Flahault, F 34060 Montpellier Cedex 1, France.

colipase was reported to act as a satiety signal in rats for fats (Erlanson-Albertsson & Larsson, 1988; Erlanson-Albertsson et al., 1991).

The sequence of colipase proves to be well conserved among different species (Fig. 1) (Erlanson-Albertsson, 1992). The 10 cysteines, all engaged in disulfide bridges, are absolutely conserved, as well as a hydrophobic region (residues 53–59) containing three tyrosines. Spectroscopic evidence exists for the involvement of these tyrosines in lipid binding (Cozzone et al., 1981).

The recently determined X-ray structures of pancreatic lipase–colipase complexes have shown that colipase binds exclusively to the noncatalytic C-terminal domain of pancreatic lipase in the absence of substrates or inhibitors (van Tilbeurgh et al., 1992, 1993a). Upon binding of substrate, two surface loops of pancreatic lipase covering the active site undergo drastic conformational changes. The rearrangement of one of these loops, the lid, creates a second binding site for colipase; in the open form of the complex, the N-terminal region of colipase interacts with the catalytic domain of lipase. These results also demonstrate that the structure of colipase is very well adapted for its function: two hydrophilic turns interact with lipase while the hydrophobic tips of its four fingers form the lipid-binding site.

The three-dimensional structure of the complex, based on 3-Å-resolution data, revealed some disagreement with biochemical results. The crystallographically observed disulfide bridges did not correspond to those deduced from biochemical experi-

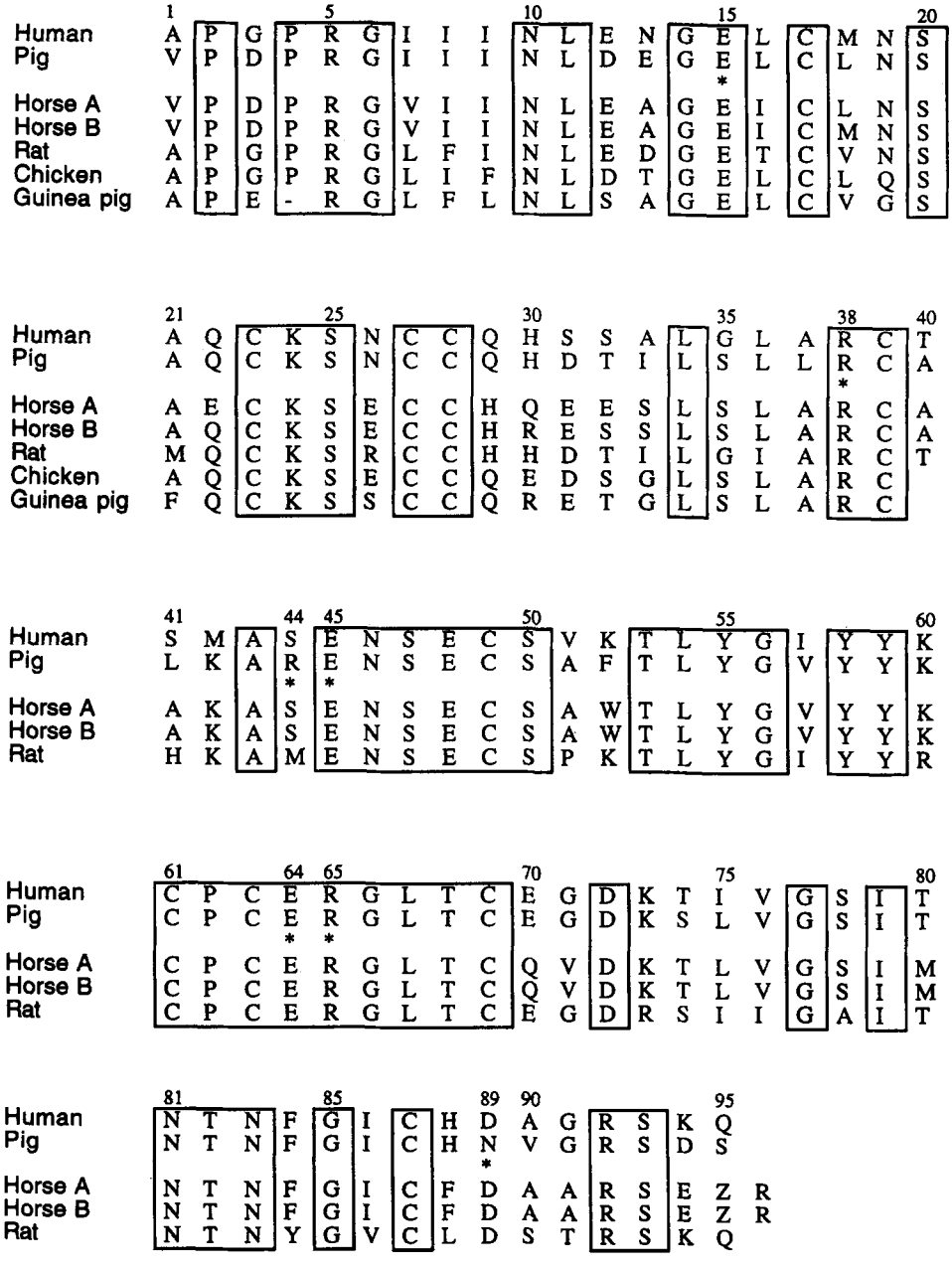

Fig. 1. Sequence alignment of different colipases. Residues interacting with lipase are indicated with *.

ments (Erlanson et al., 1974) and the colipase-binding site on the C-terminal domain of pancreatic lipase is different from the site that was extrapolated from chemical crosslinking experiments (Chaillan et al., 1992). In this paper we use the 2.4-Å-resolution crystal structure of a covalently inhibited colipase–lipase complex to give an accurate description of the colipase structure and of its interactions with pancreatic lipase (see Kinemage 1). The refinement of some bound detergent molecules in this crystal form gives us some experimental observation on how the complex interacts with the lipid/water interface.

Results

Quality of the structure

Data on the present crystal form of the complex between colipase and covalently inhibited lipase have been collected to 2.46 Å resolution. The overall thermal *B*-factors of colipase, which are 42 Å^2 and 44 Å^2 for the main and side chains, respectively, are considerably higher compared to the corresponding values of 28 Å^2 and 29 Å^2 for lipase. This may be due to a global disorder of the complex and/or to the high mobility of certain regions in the colipase molecule (see Discussion). The validity of the colipase model can be evaluated from the Ramachandran plot (Fig. 2) and from the refinement statistics, calculated for the colipase alone. The majority (81.6%) of the residues are situated inside the most favored regions of the Ramachandran plot. The remaining residues are all located in the additional allowed region as defined in Procheck (Laskowski et al., 1993). Some asparagines (Asn 10, Asn 46, and Asn 81) are found in the α_L-region and are situated in sharp β-turns. The RMS deviation from ideal bond lengths is 0.011 Å and from ideal bond angles is 1.9° (values for colipase alone). The final model contains coordinates for 85 residues (residues 6–90). The last three C-terminal residues (Gly 91, Arg 92, and Ser 93) are not visible in the electron density map and consequently are not included in the model. The three regions consisting of the tips of the finger-like loops (residues 31–35, residues 51–55, and residues 71–79) have the highest *B*-factors and are the less well-defined areas within the molecule. Meanwhile, the definition of the electron density in these regions is much better than that of the 3.0-Å-resolution structure of the closed pancreatic lipase–colipase complex (van Tilbeurgh et al., 1992) and it makes it possible for us to improve the quality of our model. Figure 3A and B show the $2F_o - F_c$ residual electron density map for a well-defined (residue 43–48) and for a less well-defined region (residues 53–56).

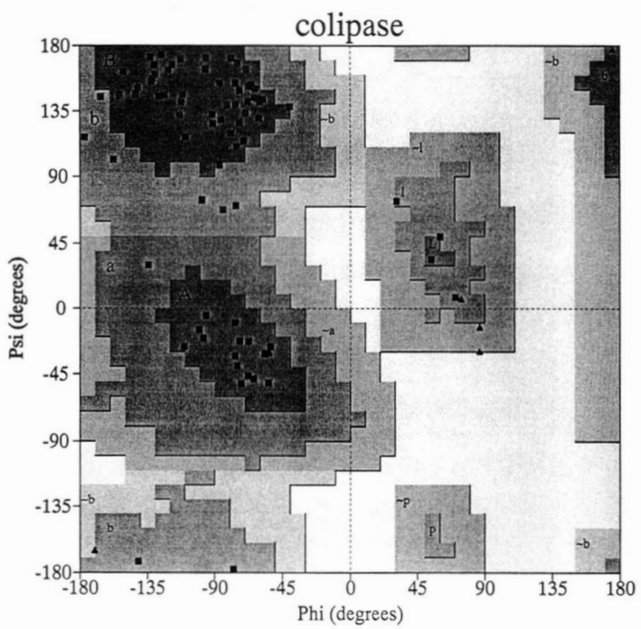

Fig. 2. Ramachandran plot output from Procheck. Glycine residues are plotted with a triangle; all others residues are marked with a square.

The 3.0-Å-resolution structure has shown that three of the five disulfide bridges were wrongly assigned according to biochemical analysis. The present 2.46-Å-resolution structure confirms the earlier crystallographic assignment. We initially refined the structure using the 3.0-Å-resolution coordinates, in which we replace the 10 cysteines by alanines. The presence of strong peaks in the Fourier difference map after refinement clearly indicates the position of our disulfide bridges. The position of these disulfide bridges is also confirmed by the structure of the homologous ternary complex between human pancreatic colipase, human pancreatic lipase, and the C11P inhibitor (unpubl. results). The $2F_o - F_c$ electron density for one of the chemically misassigned disulfide bridges (Cys 63–Cys 87) is shown (Fig. 3C). Coordinates have been deposited in the Brookhaven Protein Data Bank (Entry 1LPB).

Secondary and tertiary structure

The structures of colipase reported at 3.0 Å resolution reveal no important differences with the present higher resolution model (van Tilbeurgh et al., 1992, 1993a). Colipase is a flattened molecule of overall dimensions 25 × 30 × 35 Å (Kinemage 1). Four fingers protrude from a compact core held together by a network of disulfide bridges. Procolipase belongs to the family of small cysteine-rich molecules that lack regular secondary structure and hence defined topology. The Ramachandran plot (Fig. 2) shows that the majority of residues are in the β-region, but only short stretches of β-sheet are formed. Only two short peptides are found in the α-helical region (residues 20–22 and residues 75–80). The latter is situated at the tip of one of the most mobile finger and has very high temperature factors. Some isolated residues with α-helical dihedral angles are found in the turns (Table 1).

A Cα backbone diagram of the superposed colipase structures at 3.0 Å and 2.4 Å is shown in Figure 4. The four fingers, of unequal length, are connected by β-turns containing hydrophilic residues. Finger 1 (residues 14–23) is in random coil and contains a short stretch of α-helical residues (residues 22–24). Finger 1 is connected to Finger 2 (residues 27–39) by a type I β-turn (residues 23–26). Finger 2 is made by two elongated strands of unequal length (residues 27–31 and 35–43) with a sharp hydrophobic type I β-turn in between (residues 32–35). Finger 3 (residues 47–64) harbors the three tyrosines. It is contained between two β-turns that define the main interaction site of colipase with the C-terminal domain of lipase (residues 44–47 and 64–67). The fourth and last finger is the longest and comprises residues 68–88.

Only few main-chain hydrogen bonds exist between the individual fingers (Table 1). The majority of these hydrogen bonds are between residues that are close to the disulfide bridges. These

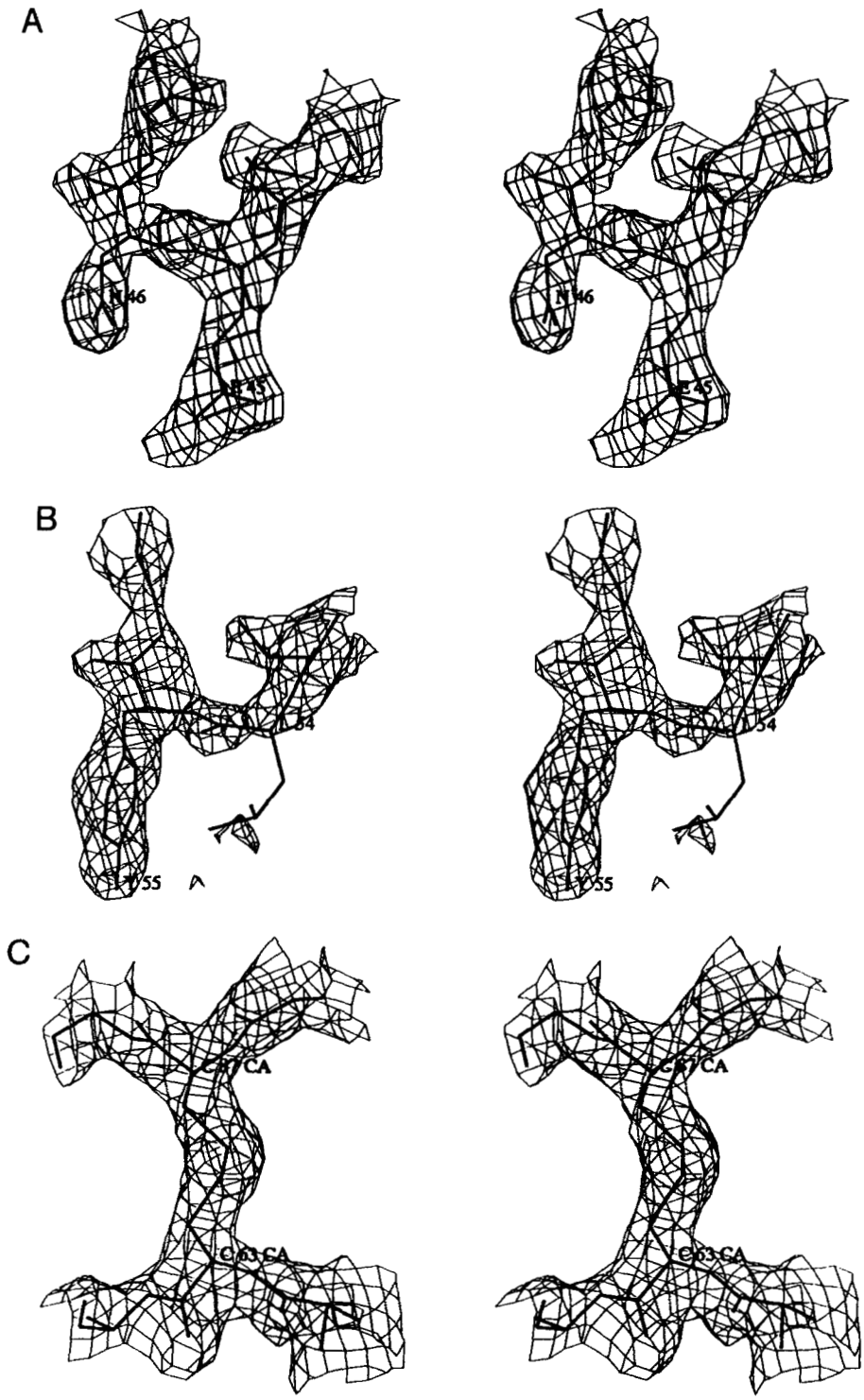

Fig. 3. Stereographic views of the 1σ contour of a $2F_o - F_c$ electron density map of **(A)** the region between residues 43 and 48, **(B)** the region between residues 53 and 56, and **(C)** the Cys 63–Cys 87 disulfide bridge.

disulfide bridges seem to be the main stabilizing factor of the colipase structure. Every disulfide bond forms a bridge between different fingers, close to the lipid-bonding site (Fig. 5; Kinemage 1). This disulfide network extends across the molecule and is mainly situated close to the lipase-binding site. Four of the disulfide bonds are paired two by two. Cys 17–Cys 28 and Cys 23–Cys 39 cross each other almost perpendicularly and their sulfur atoms are at van der Waals distance. The same observation holds for the disulfide pair Cys 63–Cys 87 and Cys 49–Cys 69 (Fig. 6A,B). The fifth disulfide bridge (Cys 27–Cys 61)

Table 1. *Structural analysis of colipase by residue*

Residue	Dihedral angles		Main-chain hydrogen bonds (Å)		Region of Ramachandran plot[a]	*B*-factors (Å^2) main chain (side chain)	Accessibility (Å^2) (secondary structure[b])
	ϕ	ψ	C=O	N			
G6						69 (0)	
I7					l	66 (73)	176
I8	−176	116			b	59 (62)	98
I9	−95	171	I9	L11(3.20)	B	50 (50)	121
N10	54	34			L	43 (46)	112 (S)
L11	−65	153	L11	K24(3.07)	B	36 (33)	6 (B)
D12	−95	164	D12	E15(3.00)	B	39 (48)	74 (t)
E13	−59	141			B	34 (39)	92 (B)
G14	86	−13			–	34 (0)	50 (T)
E15	−81	139	E15	C39(2.84)	B	34 (39)	90 (t)
L16	−63	150			B	32 (24)	82 (B)
C17	−150	162			B	29 (31)	5
L18	−110	−26			A	34 (33)	122 (S)
N19	−153	145	N19	A21(2.98)	B	34 (42)	65 (g)
				Q22(2.91)			
S20	−53	−26	S20	Q22(3.05)	A	38 (34)	14 (G)
				C23(2.99)			(G)
A21	−56	−31			A	41 (42)	65 (G)
Q22	32-73	−22	Q22	L11(2.81)	A	44 (38)	16 (B)
C23	−91	132	C23	S25(3.29)	B	41 (36)	1 (S)
K24	−54	−51	K24	N26(3.26)	A	45 (46)	107 (S)
S25	−79	119	S25	C27(2.63)	B	43 (34)	14 (S)
N26	−75	70	N26		b	40 (59)	85 (S)
C27	−157	101	C27	A40(2.98)	b	33(31)	0 (e)
C28	−91	126	C28	Y58(3.02)	B	33 (36)	0 (E)
Q29	−132	155	Q29	R38(2.91)	B	42 (40)	40 (E)
H30	−153	146			B	53 (59)	16 (e)
D31	−76	−32			A	58 (66)	125 (S)
T32	−132	172			B	61 (63)	78 (S)
I33	−64	−48	I33	S35(3.26)	A	61 (60)	122 (S)
L34	−98	74			b	62 (61)	162 (S)
S35	−166	144			b	53 (49)	48 (S)
L36	−63	144			B	41 (42)	126
S37	−112	141	S37	C17(2.91)	B	36 (34)	13
R38	−130	166	R38	Q29(2.87)	B	29 (38)	112 (E)
C39	−69	133	C39	G14(2.72)	B	26 (29)	4 (E)
A40	−131	157			B	28 (28)	25 (e)
L41	−73	149			B	32 (29)	110
K42	−67	151			B	30 (40)	60
A43	−60	129	A43	E64(3.09)	B	23 (17)	10 (B)
R44	−78	171			B	22 (25)	173 (t)
E45	−57	143			B	21 (24)	86 (T)
N46	70	7			l	30 (33)	104 (T)
S47	−112	171	S47	C87(2.96)	B	33 (30)	42 (e)
E48	−67	141			B	41 (43)	122 (E)
C49	−141	−172			b	44 (39)	0 (E)
S50	−141	150			B	45 (43)	1 (E)
A51	−76	139	A51	T53(3.28)	B	61 (59)	15 (e)
F52	−40	137			B	73 (82)	175
T53	−125	173			B	72 (74)	14
L54	−100	−15			A	75 (81)	122 (S)
Y55	−76	−10	Y55	V57(3.16)	A	65 (67)	119 (S)
G56	86	−30	G56	S20(2.98)	–	48 (0)	10 (e)
V57	−120	163			B	46 (43)	24 (E)
Y58	−129	160	Y58	H30(3.01)	B	41 (31)	11 (E)
Y59	−97	−20			A	28 (49)	43 (S)
K60	−142	146			B	28 (42)	52 (S)
C61	−86	154	C61	S50(3.20)	B	30 (30)	10
P62	−69	163	P62	A43(2.85)	–	27 (27)	18

(*continued*)

Table 1. *Continued*

Residue	Dihedral angles		Main-chain hydrogen bonds (Å)		Region of Ramachandran plot[a]	*B*-factors (Å^2) main chain (side chain)	Accessibility (Å^2) (secondary structure[b])
	ϕ	ψ	C=O	N			
C63	−74	168			B	29 (30)	17 (B)
E64	−77	−177	E64	L67(3.22)	b	28 (31)	95 (t)
R65	−61	143	R65	L67(3.21)	B	28 (34)	237 (T)
G66	74	5			–	27 (0)	66 (e)
L67	−111	146			B	27 (21)	32 (E)
T68	−113	131	T68	H88(2.78)	B	31 (32)	64 (E)
				E70(3.15)			
C69	−86	97			b	35 (34)	21 (E)
E70	−85	128	E70	I86(2.82)	B	36 (49)	88 (E)
G71	175	177			–	51 (0)	42 (S)
D72	−73	126			B	59 (70)	155
K73	−109	116			B	62 (63)	133
S74	−118	166	S74	S78(2.96)	B	56 (58)	63 (h)
L75	−74	−39			A	56 (52)	128 (H)
V76	−67	−46	V76	S78(3.03)	A	60 (60)	91 (H)
				I79(3.05)			
				T80(2.81)			
G77	−53	−31	G77	N81(2.97)	–	61 (0)	6 (H)
				T82(2.84)			
S78	−72	−51	S78	T80(3.21)	A	58 (53)	46 (H)
				N81(3.14)			
I79	−67	−23			A	58 (58)	93 (H)
T80	−95	−5			A	51 (54)	65 (H)
N81	60	49			l	52 (57)	7 (h)
T82	−134	30	T82	F84(2.78)	a	46 (50)	61 (t)
N83	−84	67	N83	A51(2.91)	b	50 (52)	8 (e)
F84	−78	154			B	48 (37)	57 (E)
G85	−170	166	G85	C49(2.98)	–	37 (0)	12 (E)
I86	−127	145	I86	E70(2.97)	B	33 (32)	66 (E)
				H88(3.25)			
C87	−70	114	C87	N46(2.73)	B	28 (28)	0 (E)
H88	−123	145	H88	T68(2.94)	B	27 (32)	55 (E)
				V90(3.08)			
N89	−75	110			B	32 (35)	106 (E)
V90					b	48 (48)	138 (e)

[a] Region of the Ramachandran plot: A, core α; a, allowed α; B, core β; b, allowed β; L, core left-handed α; l, allowed left-handed α; p, allowed ϵ; XX, outside major areas.

[b] Secondary structure (extended Kabsch/Sander): B, residue in isolated β-bridge; E, extended strand, participates in β-ladder; G, 3-helix (3/10 helix); H, 4-helix (α-helix); I, 5-helix (π-helix); S, bend; T, hydrogen bonded turn; e, extension of β-strand; g, extension of 3/10 helix; h, extension of α-helix.

is situated in the middle of the molecule and connects the two halves (Fig. 5).

Interactions with lipase

Colipase mainly interacts with the C-terminal domain of lipase (see Kinemage 1). A detailed list of the polar contacts between lipase and colipase can be found in Table 2. Residues of two hairpin loops, connecting fingers 2 and 3 (44–47) and fingers 3 and 4 (64–67), are involved in the interactions with lipase. The folding of colipase brings these loops close together onto the protein surface. The first and second residue of the first turn make polar contacts with lipase (Fig. 7A): Arg 44 makes a salt bridge with Asp 389 and Glu 45 with Lys 399. The main-chain carbonyl oxygen of Glu 45 also hydrogen bonds to the side-chain amido group of Asn 365. The two following residues of this turn have no direct polar contacts with lipase. A similar situation occurs for the interaction between lipase and the second turn of colipase: the carboxylate side chain of Glu 64 makes a hydrogen bond with the main-chain nitrogen of Gln 368 and the main-chain carbonyl oxygen of Arg 65 hydrogen bonds to the side chain of Gln 368. Finally, a hydrogen bond exists between the OD1 atom of Asn 89 of colipase and the NZ atom of Lys 399 of the C-terminal domain of lipase. The interacting turns of colipase are held firmly into place by the disulfide bridges, which are situated next to them.

The structure of the ternary lipase–colipase–phospholipid complex has shown that the rearrangement of the active-site lid

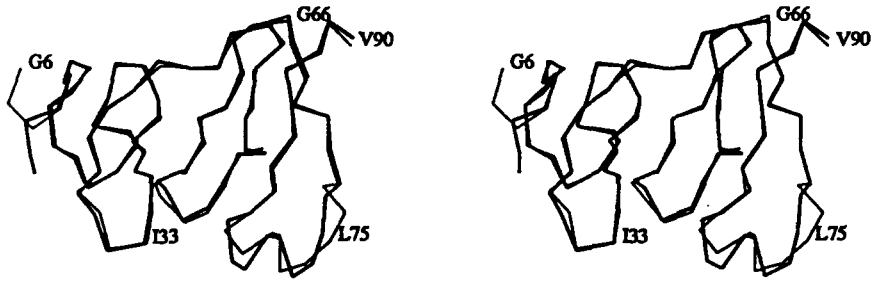

Fig. 4. Stereographic view of the superposition of the 3.0-Å (in thick lines) and 2.46-Å (in bold lines) Cα structures of the colipase.

of lipase upon substrate binding creates a second binding site for colipase (van Tilbeurgh et al., 1993a; Egloff et al., 1995). Due to this conformational change, the minor α-helix of the open lid is facing the N-terminal part of colipase. This second colipase-lipase-binding site is smaller than the one described above and contains fewer contacts. In this region, three hydrogen bonds are observed: the first between OE1 of Glu 15 of colipase and the main-chain N of Asn 240 of the lid, and the second and the third between, respectively, Arg 38 NH1 and and the main-chain carbonyl of Val 246 and Arg 38 NH2 and the same main-chain carbonyl of Val 246 (Fig. 7B; Kinemage 1). In total, colipase forms 11 direct hydrogen bonds with lipase, 3 with the lid and 8 with the C-terminal domain.

Colipase also makes numerous van der Waals contacts with lipase. There are 28 contacts shorter than 4 Å between the N-terminal region of colipase and the lid and about 80 contacts between colipase and the lipase C-terminal domain. The total surface of interaction between lipase and colipase is 950 Å^2: the 612-Å^2 interaction surface shared by colipase and the C-terminal domain of lipase add to the 338-Å^2 surface of interaction between colipase and the N-terminal domain of lipase.

The interaction between lipase and colipase is not entirely mediated by direct protein-protein contacts. Some well-defined water molecules that bridge side chains from lipase and colipase are clearly observed in the electron density (Table 3). The very well-defined water molecule 13W bridges the two β-turns of colipase and lipase (hydrogen bonds to Glu 45 and Glu 64 of colipase and to Ser 366 of lipase). Another important water (1W) is in a network with β-turn 2 (Gly 66), the C-terminal interacting residue of colipase (Asn 89) and lipase (Leu 443). A third one (138W) bridges the main-chain carbonyl of Gly 14 and the side chain of Arg 38 of colipase to two main-chain oxygen atoms of two residues of the lid (Ser 243 and Val 246). Three more water molecules bridge colipase to lipase.

The two turns and the C-terminus of colipase do not form a contiguous binding site. Figure 8 and Kinemage 1 show that the contact zone between lipase C-terminal domain and colipase contains a cleft. Another obvious discontinuity exists between the two different binding sites, creating a large hole in the complex. The wall of this hole is lined with a high number of charged residues.

Lipid interaction site

A number of detergent molecules (β-octylglucoside) were observed in the crystal and two of them interact with colipase (see Kinemage 1). The sugar part of the first one makes two hydrogen bonds and is 34 contacts shorter than 4.0 Å with colipase. The second β-octylglucoside molecule is bound to colipase via only one hydrogen bond. The glucose ring also makes polar contacts with the N-terminal domain of the lipase. The hydrophobic tail of this molecule lies against the second colipase finger, also making a number of van der Waals contacts (Fig. 9). Previous trials of soaking and cocrystallization with bile salts or phospholipids failed to detect these amphipathic molecules bound to colipase. The asymmetric partition of hydrophilic and hydrophobic residues on the colipase surface suggests the regions of colipase that may be important for binding to the lipid/water interface. The majority of hydrophobic residues of colipase are situated on the face opposite the interaction site with the C-terminal domain of lipase (Egloff et al., 1995). We therefore propose that the interaction of colipase with the lipid/water interface takes place through the following residues: N-terminus (Ile 7, 8, and 9), finger I (Leu 16, Leu 17), finger II (Ile 33,

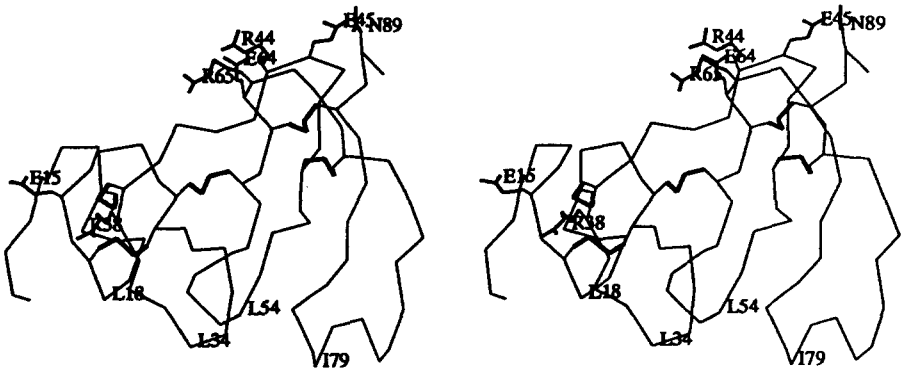

Fig. 5. Stereographic diagram of the three-dimensional structure of colipase as determined in the ternary complex HPL-Pcol-C11P. Disulfide bridges are shown in bold lines. Residues with side chains are those interacting with lipase in the ternary complex.

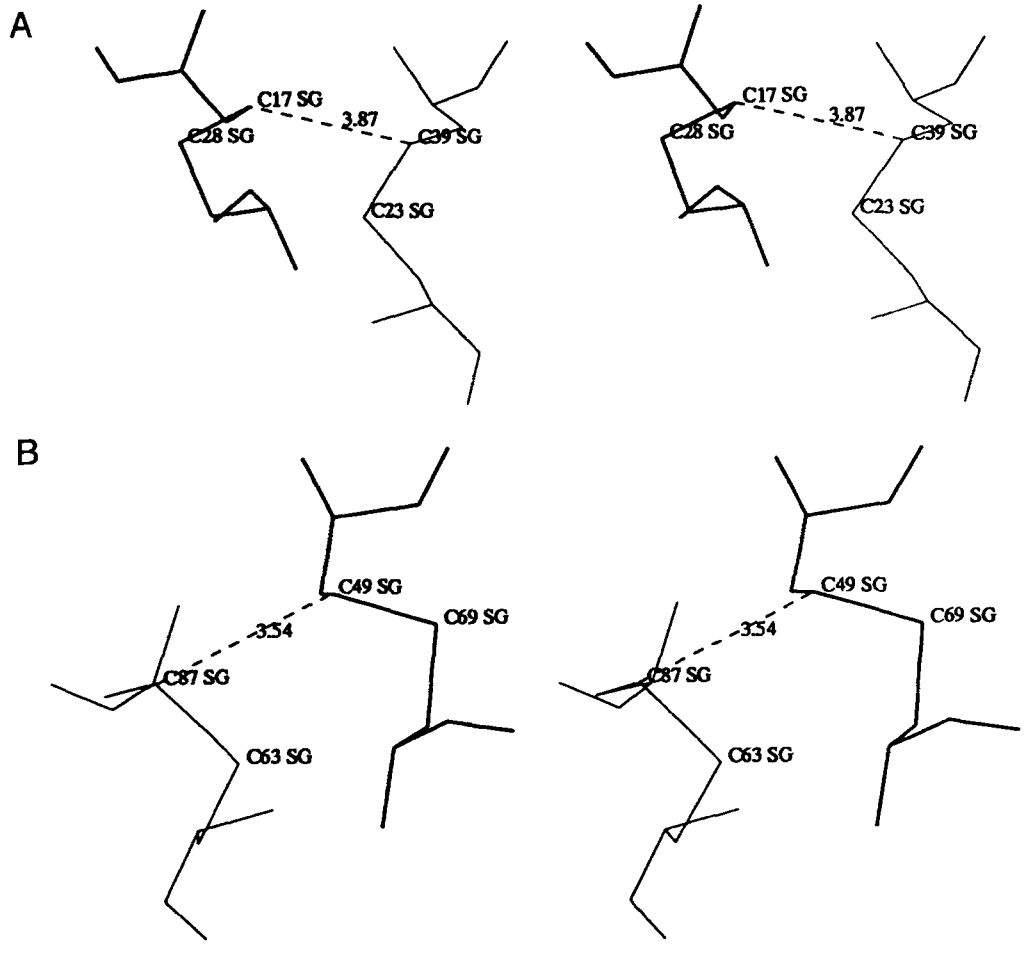

Fig. 6. Stereographic view of (**A**) the first pair of disulfide bridges: Cys 17-Cys 28 and Cys 23-Cys 39; and (**B**) the second pair of disulfide bridges: Cys 63-Cys 87 and Cys 49-Cys 69.

Leu 34, and Leu 36), finger III (Leu 54, Tyr 55, Val 57, Tyr 59), and finger IV (Leu 75, Val 76, Ile 79, and Phe 84). These residues form a hydrophobic plateau that is a continuation of the hydrophobic surface of the open lid of lipase (van Tilbeurgh et al., 1993a; Egloff et al., 1995). The hydrophobicity of all these residues, except Ile 33, is conserved among the different species.

Table 2. *Polar contacts between lipase and colipase*

Atoms belonging to colipase	Atoms belonging to lipase	Distance (Å)
Glu 15 OE1	Asn 240 N	2.78
Arg 38 NH1	Val 246 O	2.44
Arg 38 NH2	Val 246 O	2.94
Arg 44 NH1	Asp 389 OD1	2.87
Arg 44 NH1	Asp 389 OD2	2.79
Arg 44 NH2	Asp 389 OD1	2.93
Glu 45 OE1	Lys 399 NZ	2.75
Glu 45 O	Asn 365 ND2	2.98
Glu 64 OE1	Gln 368 N	3.16
Arg 65 O	Gln 368 NE2	3.02
Asn 89 OD1	Lys 399 NZ	2.98

Comparison of colipase in the various complexes

Three structures of lipase-colipase complexes have now been solved. The first crystallized in the trigonal space group $P3_121$ and did not contain lipid. The second one crystallized in the presence of mixed micelles of bile salts and phospholipid in space group $P4_22_12$. The present crystal form is isomorphous to the previous one, and the lipase is covalently inhibited by a phosphonate inhibitor (Egloff et al., 1995). We superposed the coordinate sets of the colipase from the three complexes and conclude that they are very similar. The fact that colipase was constructed independently in two of these structures demonstrates their validity (van Tilbeurgh et al., 1993a). The RMS difference for the Cα positions of the three colipase structures is between 0.39 and 0.49 Å for residues in the well-defined regions. The regions that diverge are situated in the N-terminal peptide and in the highly mobile tips of the fingers. The slightly different conformation of the N-terminal region (residues 6–9) may be explained by different packing effects in two of the complexes. In the trigonal crystal form with the lipase in closed conformation, this pep-

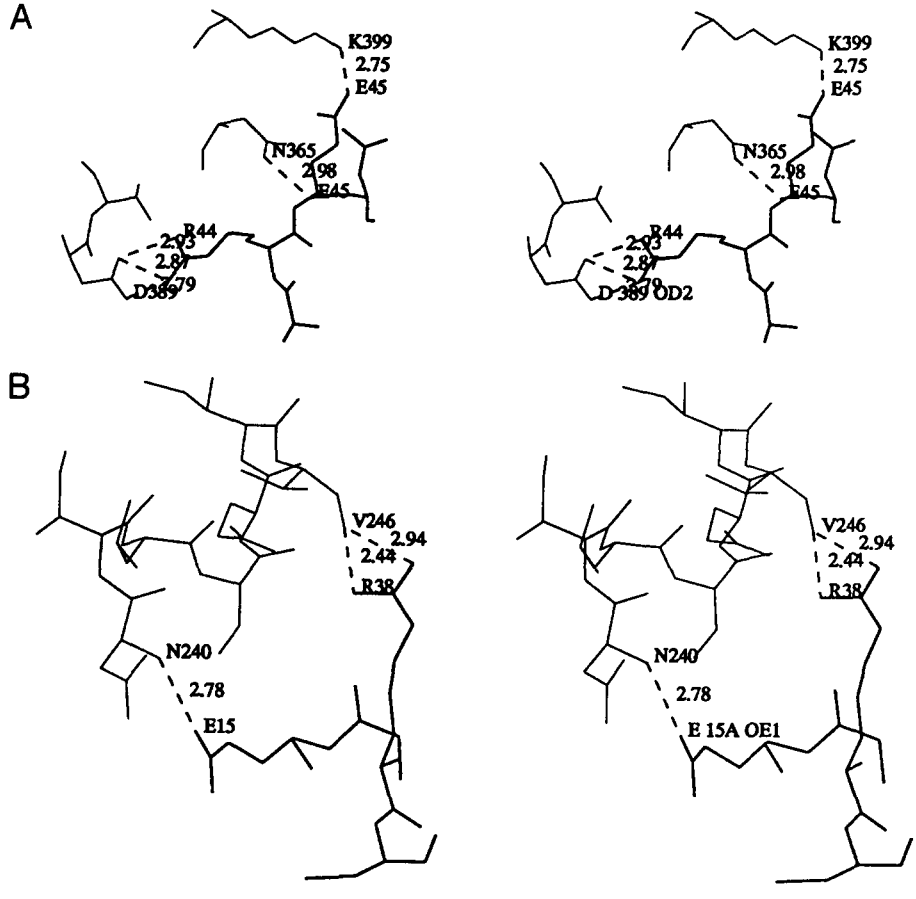

Fig. 7. Polar contacts between the colipase and (**A**) the C-terminal domain of the lipase (**B**) the lid of the lipase.

tide makes crystal contacts with a neighbor lipase molecule. In the complexes with lipase in the open conformation, the N-terminal peptide is close to the lipase lid region. The different conformations between the crystal form with micelles and the crystal form with covalent inhibitor may be explained by the fact that the first was carried out with procolipase (containing the first five residues), whereas the present structure is with trypsin-cleaved colipase. Although we never observed the N-terminal peptide in the crystal, its presence may influence the conformation of the following residues in the sequence.

The interaction between colipase and the C-terminus of lipase, as observed in all three crystal structures, is very well conserved and perfectly superposable. The interaction between colipase and the open lid, present in only two crystal structures, is also very similar.

Discussion

The considerable average *B*-factor of colipase, which is about 50% higher than for lipase, may have the following origins:

Table 3. *Bridging water molecules at the lipase-colipase binding site*

Water molecules	*B*-factor (Å^2)	Colipase	Distance between colipase and water molecules (Å)	Lipase	Distance between lipase and water molecules (Å)
1	25	G66 O	2.96	L443 N	2.71
1		N89 ND2	2.98	L443 N	
13	17	E45 N	2.76	S366 O	3.03
13		E64 OE2	2.70	S366 O	
30		N89 ND2	2.83	L443 O	2.86
136	36	E45 OE1	2.57	K399 NZ	2.88
138	29	G14 O	3.15	S243 O	2.82
138		R38 NH1	2.43	V246 O	2.96
273	65	E13 O	3.15	D331 OD1	3.08

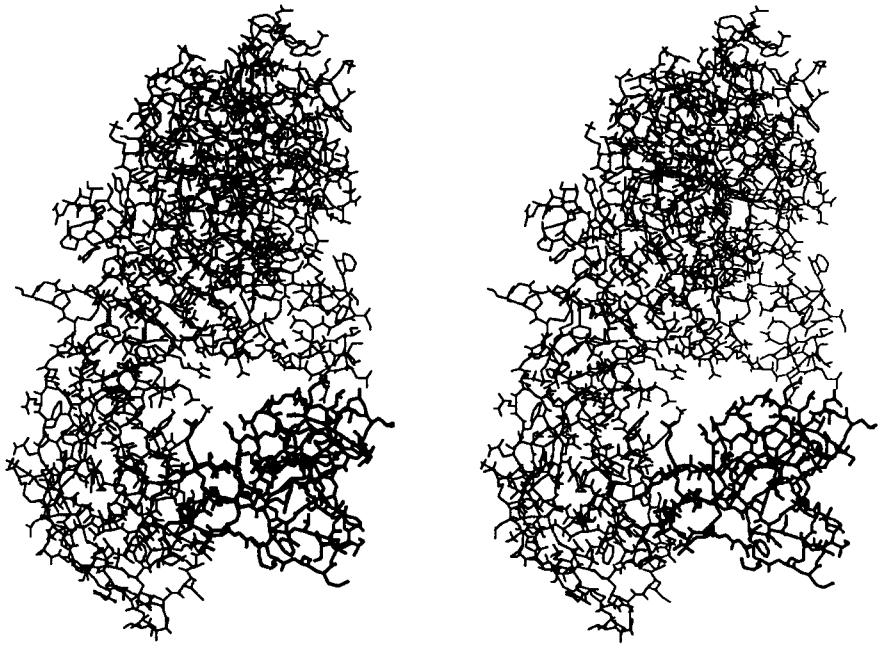

Fig. 8. Stereographic view of the contact zone between the C-terminal domain of the lipase and the colipase.

(1) the observed crystal structure is an average of a family of closely related but slightly different complexes; and (2) an important part of the colipase molecule is not engaged in inter- or intra- (with lipase) molecular hydrogen bonds and is therefore very mobile. The affinity of lipase and colipase is reported to be low in solution (5×10^5 M^{-1}), but increases a few orders of magnitude (10^9-10^{10} M^{-1}) in the presence of a lipid/water interface (Sternby & Erlanson-Albertsson, 1982). It is difficult to guess what the intrinsic increase in affinity is because the binding constants determined in a heterogenous system are imperatively apparent. However, even bound to an interface, the lipase-colipase complex can be classified among the low average affinity protein-protein complexes. An analogous discrepancy between the *B*-factors of the partners in a protein-protein complex was observed in the thrombin-hirudin structure. Although the affinity constant of the complex is on the order of 10^{-14} M, the observed *B*-factors of hirudin were about 50% higher than for thrombin (Rydel et al., 1991). The regions of colipase interacting with lipase have *B*-factors comparable to those of pancreatic lipase, suggesting that the high average *B*-factors are due to the mobility of the tips of the fingers. Another factor that may influence global *B*-factors are crystal packing effects. Colipase is devoid of crystal contacts in the present crystal form and this may also contribute to the higher *B*-factors.

Colipase belongs to the family of small cysteine-rich proteins that lacks well-defined secondary structure elements (Alder et al., 1991; Saudek et al., 1991). From the discovery of colipase on, it was proposed that this protein contains two functional regions: a lipase-binding region and a lipid-binding region. The various crystal structures that have been solved confirm this early hypothesis and establish the various regions of the sequence involved in these functions. Colipase mainly binds to the C-terminal region of lipase and that is probably the sole interaction between lipase and colipase in the absence of a lipid/water interface. The small surface covered by that interaction, about 600 $Å^2$, and the limited number of hydrogen bonds (eight distances less than 3.2 Å) explain why this binding is weak ($K_{ass} \approx 5 \times 10^5$ M^{-1}). Nevertheless, the function of the lipase-colipase pair rests

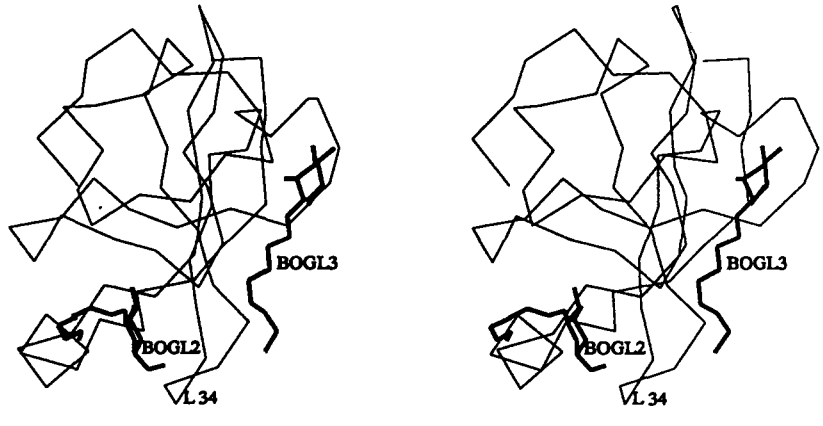

Fig. 9. Stereographic view of the two β-octylglucoside molecules interacting with colipase. The second finger of colipase is flanked by the glucose ring of one molecule and the hydrophobic tail of the second one.

upon a specific 1:1 complex formation (Borgström & Erlanson-Albertsson, 1984). The binding sites of both the C-terminal lipase domain and colipase are discontinuous and involve about 13 lipase and 9 colipase residues. The interaction between lipase an colipase seems to be mainly hydrophilic. An important number of van der Waals contacts may contribute to binding: especially the stacking of Tyr 403 of lipase and Arg 65 of colipase provides an important number of contacts. The C-terminal domain of lipase binds as a rigid entity onto colipase. Conformational changes were not expected in this region because it is situated in the center of a β-sheet. Moreover, the region of colipase involved in the binding to lipase seems to be rather rigid because it is stabilized by a few neighboring disulfide bridges (Cys 87/Cys 63; Cys 69/Cys 49). Because no structure of colipase is available in the absence of lipase, we do not know whether there are any structural changes induced upon lipase binding.

When a substrate is bound to the active site of lipase, the lid undergoes drastic conformational modifications (van Tilbeurgh et al., 1993a; Egloff et al., 1995). As a result, colipase is enclosed in pincers formed by the N- and C-terminal domains of lipase. The second binding site, 25 Å removed from the C-terminal domain binding site, adds 300 $Å^2$ to the total interaction surface. The lid makes three additional hydrogen bonds with colipase and one water molecule (W 138) is bridging 2 residues of the lid and 2 residues of the colipase (Table 3). This extra binding site may explain why the apparent affinity of lipase and colipase increases in the presence of a lipid/water interface. The total interaction surface and the number of hydrogen bonds are in the range of those of other protein–protein recognition sites (Janin & Chothia, 1990). The importance of the interaction between colipase and the lipase lid for the functioning of the complex is not known. Chemical modification studies of colipase demonstrated the importance of two carboxylate groups, Glu 15 and Asp 72, in the activation process. Immunochemical studies have provided evidence that only Glu 15 is involved in the interaction (N. Rugani, pers. comm.). In our structure, Asp 72 is actually far removed from the lipase-binding sites and can therefore be discarded, confirming that Glu 15 is the important carboxylate for lipase recognition.

The available sequences of procolipase (Fig. 1) display a high degree of homology (72 residues identical between human and porcine colipase). No important deletions nor insertions are observed in any of the species. Most of the substitutions are conservative. Thus, one may safely conclude that all colipases will have almost identical three-dimensional structures. This is confirmed by the three-dimensional structure of the same complex using human recombinant pancreatic procolipase instead of porcine colipase (unpubl. results). Biochemical studies have shown that not all of the colipase sequence is needed for activation of lipase. The first five amino acids of procolipase are cleaved by trypsin without affecting the efficiency of colipase. The resulting pentapeptide, called enterostatin, has been shown to reduce fat intake selectively (Erlanson-Albertsson & Larsson, 1988; Erlanson-Albertsson et al., 1991). In previously reported structures of the pancreatic lipase–procolipase complex, we did not observe electron density for this peptide. This indicates that it is very mobile and is compatible with the sensitivity to proteolysis. The present structure is with colipase lacking the N-terminal peptide. As expected, the N-terminal peptide does not influence the overall conformation and binding mode of colipase. Some differences are observed however in the conformation of the N-terminal residues 6–9 between colipase and procolipase. This region probably adopts multiple conformations in the present structure. Colipase can also be trimmed at the C-terminus without loss of activity. The length of colipase may vary upon species and preparations (Rugani, 1993). We never observed any electron density beyond residue 90. The C-terminal peptide apparently does not bind to lipase and is also remote from the presumed lipid-binding site. This may explain why colipase activity is not sensitive to partial proteolysis at the C-terminus.

The activation by colipase is specific for pancreatic lipases; microbial lipases that are bile salt inhibited are not reactivated (Canioni et al., 1977) by colipase. Pancreatic lipase from one species can be activated by colipase from other species (Rathelot et al., 1981; Sternby & Borgström, 1981). Comparison from the colipase sequence alignments of the residues that interact with lipase (Fig. 1) shows that most of them are conserved within the colipase family. The two residues that make hydrogen bonds with the lid are absolutely conserved (Glu 15, Arg 38). The most important nonconservation of a residue interacting with lipase is situated in the first interacting β-turn, where Arg 44 of porcine colipase is substituted by serine in equine, human, and canine colipases (Fukoa et al., 1990, 1993; Renaud & Dagorn, 1991) and by methionine in rat. Interestingly, Arg 44 makes a charged hydrogen bond to Asp 389, which is the only lipase residue that hydrogen bonds to colipase and that is not absolutely conserved in the lipase family. The recently solved structure of the human pancreatic lipase–human procolipase complex shows that colipase binds identically to lipase as in the present hybrid human/porcine complex (Egloff, 1995). Slight structural rearrangements are sufficient to accommodate for varying side chains at position 44 of colipase. The second and last colipase residue that makes a hydrogen bond with lipase, but that is not absolutely conserved, is Asn 89. This residue is aspartate in all other sequences. In the human pancreatic lipase–human procolipase complex, this interaction between Asn 89 of colipase and Lys 399 of lipase is not conserved.

The second important functional site of colipase is the lipid/water interface binding site. It has been reported that colipase alone is capable of binding to lipid substrates and bile salt micelles (Sternby & Erlanson-Albertsson, 1982; McIntyre et al., 1987). Although we never observed bile salts or phospholipids bound to colipase in the crystals, reasonable predictions about the interface binding site of colipase can be made from the structure of the lipase–colipase complex. The tips of the fingers are opposite to the lipase-binding site and contain an unusually high number of exposed hydrophobic residues (van Tilbeurgh et al., 1993a). The N-terminal peptide contains three successive hydrophobic residues (Ile 7, 8, and 9) that are close to the hydrophobic surface of the open lipase lid. We proposed that the lipid-binding site is made by the tips of the hydrophobic fingers and by the N-terminal peptide (van Tilbeurgh et al., 1993a). Together with the hydrophobic surface surrounding the active site of lipase, they make a 50-Å-long plateau particularly apt to bind onto a hydrophobic surface. Successive removal of three N-terminal isoleucines of porcine procolipase results in the loss of the binding capacity to Intralipid (Kabi-vitrum, Stockholm), a mixture of soy triglycerides and lecithin (Erlanson-Albertsson & Larsson, 1981). These residues are substituted by similar hydrophobic residues in the other known sequences. This peptide is situated next to the hydrophobic face of the lipase lid, suggesting that it is also involved in interface binding. The first fin-

gertip is the least hydrophobic, containing only one hydrophobic residue (Leu 18, Met, or Val). The second tip is a β-turn comprising Ile 33 and Leu 34, residues not frequently found in turns. Leu 34 is absolutely conserved, but Ile 33 can be Ser, Ala, or Gly. The third finger is the highly conserved "tyrosine loop" (residues 52–59). This finger is at the center of the molecule and is delimited by the two turns that bind to the C-terminal domain of lipase. Much of the early spectroscopic work on colipase concentrated on this region and especially on its three tyrosines (Cozzone et al., 1981; McIntyre et al., 1990). In the porcine colipase structure, three of the four aromatic residues (Phe 52, Tyr 55, and Tyr 59) are oriented toward the outside of the loop, whereas Tyr 58 points toward the interior of the molecule. McIntyre et al. (1990) succeeded in selectively dansylating Tyr 55 and Tyr 59. The two modified colipases retained 200% and 80% activity, respectively. Fluorescence anisotropy decay experiments of the dansylated products indicated that Tyr 55 is located on the surface and that it is totally free to rotate. Similar experiments suggested that Tyr 59 is located near the surface but has a restricted rotational freedom. These data are in agreement with our crystal structure in which the side chains of Tyr 55 and Tyr 59 are at the surface. No electron density was observed for Tyr 55, indicating that it is highly mobile. McIntyre et al. (1990) also observed that the reactivity for modification of the tyrosines follows the order 55 > 59 > 58, which corresponds to the increase of accessible surface area for the three tyrosines: Tyr 55 (119 Å^2, assuming it is totally accessible), Tyr 59 (43 Å^2), and Tyr 58 (11 Å^2). The fluorescence spectrum of colipase dansylated at Tyr 55 (blue) shifts drastically upon bile salt micelle binding, indicating a movement toward a more hydrophobic environment. This tyrosine is at the very tip of the third finger and probably penetrates into the interface. Phe 52 is substituted by Trp in equine colipase, but by Lys in human, murine, and canine colipase, meaning that an aromatic residue is not absolutely required at this position. Phe 52 is situated somewhat closer to the base of the third finger compared to Tyr 55 and Tyr 59. Finally, the tip of the fourth and last finger is made of a badly defined helical turn. This finger also contains a number of well-defined hydrophobic residues (Leu 75, Val 76, Ile 79, Phe 84).

Concluding remarks

The tips of the four fingers of colipase are very hydrophobic, which confirms previous studies in solution. They make a continuous hydrophobic plateau that is prolonged by the hydrophobic residues exposed by the opening of the flap of the lipase. This 50-Å-long hydrophobic plateau is supposed to interact with the lipid interface. Located at the opposite of the fingers, the core of colipase is much less hydrophobic and is better defined in density. This may be due to stabilization through its interaction with lipase C-terminal domain and through the network of the five disulfide bridges. Three of these five disulfide bridges were biochemically misassigned in solution (Chaillan et al., 1992) but were confirmed by NMR studies (Kaptein, pers. comm.). Such a discrepancy was recently reported for the *Ascaris* chymotrypsin/elastase inhibitor, for which disulfide bridges found both by NMR and X-ray agree but disagree with biochemical studies (Grasberger et al., 1994; Huang et al., 1994). Finally, although the complex reported here is heterologous (human/porcine), data fit well with biological studies. This structure is also confirmed by the structure of the human/human complex (Egloff, 1995).

Materials and methods

Compounds and crystallization

The present structure of the ternary complex was obtained with colipase cleaved at the N-terminus by trypsin (Rathelot et al., 1988). Crystals were obtained by mixing 8 mg/mL human pancreatic lipase (DeCaro et al., 1977) with 2.5 mg/mL porcine activated colipase (Canioni et al., 1977). The phosphonate inhibitor, the *O*-(2-methoxyethyl)*O*-(*p*-nitrophenyl)*n*-undecylphosphonate (C11P) was dissolved in THF (tetrahydrofuran) and added to the lipase–colipase solution in a molar excess of inhibitor versus lipase of 100. Sitting drops were formed with 4 μL of this mixture and 4 μL of the mother liquor after 30 min of incubation. The mother liquor contains 2% polyethylene glycol 8000 (PEG8000), 0.1 M 2-(*N*-morpholino)ethane sulfonic acid (MES) (pH 6.0), and 0.4 M NaCl. After a few days, β-octylglucoside was added to the drops. Tetragonal crystals appeared within a few hours and grew over 2 days to a maximum size of 0.5 mm × 0.5 mm × 0.5 mm. These crystals belong to the space group $P42_12$ ($a = b = 133.7$ Å, $c = 93.3$ Å). They are isomorphous with the crystals of the ternary complex lipase–colipase–phospholipid (van Tilbeurgh et al., 1993b) and data have been collected at 2.46 Å resolution.

An error in the published porcine colipase sequence was suspected on the basis of mass spectrometry experiments but was not detected in the previous 3.0-Å-resolution structure (van Tilbeurgh et al., 1993a). The leucine at position 37 should be serine as determined by N-terminal sequencing (Lars Thim, pers. comm.). The identity of serine at position 37 was confirmed by the refined electron density. Mass spectrometric analysis also indicated that the colipase used in the present study is missing two residues at the C-terminus.

Data collection and structure refinement

The X-ray data were collected on an MAR-Research Imaging plate detector with a diameter of 18 cm (Mar-reasearch, Hamburg, Germany) mounted on a Rigaku RU200 rotating anode at 40 kV × 80 mA. Data were reduced using the imaging plate version of XDS (Kabsch, 1988) and statistics are given in Table 4A and B. Structure refinement was performed using the 3.0 version of the program X-PLOR and the 3.1 version for the last cycle of refinement in order to apply the Engh–Huber force field (Engh & Huber, 1991). The initial model was composed of the lipase–colipase complex as observed in the 3.0-Å-resolution structure with the phospholipid in the active site (van Tilbeurgh et al., 1993a) without bound ligand nor water molecules. A standard protocol of simulated annealing (S.A.) was performed (Brünger & Karplus, 1991), consisting of 300 cycles of conjugate gradient minimization followed by molecular dynamics (0.5 ps at 1,500 K and 0.5 ps at 300 K), 400 steps of conjugate gradient minimization, and 15 cycles of restrained individual *B*-factor refinement. Visual inspection and manual refitting were performed between each cycle of refinement with the Turbo-Frodo software program on Silicon Graphics stations (Roussel & Cambillau, 1991).

Table 4. *Data collection and final model statistics*

Resolution shell (Å)	Number of collected reflections	Number of unique collected reflections	Number of unique possible reflections	Redundancy	Completeness (%)	R_{sym} (%)[a]	$\%I > \sigma(I)$
A. Data collection							
20.0–10.67	2,212	361	459	6.1	78.6	4.4	87.8
10.67–7.57	6,833	719	742	9.5	96.9	2.9	98.5
7.57–6.19	9,498	899	932	10.6	96.5	4.2	99.1
6.19–5.36	11,375	1,042	1,113	10.9	93.6	4.5	98.6
5.36–4.80	12,302	1,171	1,208	10.5	96.9	4.8	98.8
4.80–4.38	13,485	1,289	1,374	10.5	93.8	4.9	98.4
4.38–4.05	15,047	1,374	1,448	11.0	94.9	5.9	99.2
4.05–3.79	16,785	1,479	1,502	11.3	98.5	7.3	98.2
3.79–3.58	18,742	1,575	1,662	11.9	94.7	9.1	98.8
3.58–3.39	19,980	1,658	1,685	12.1	98.4	11.2	97.7
3.39–3.24	21,098	1,727	1,847	12.2	93.5	14.8	98.2
3.24–3.10	22,069	1,782	1,907	12.4	93.4	19.6	96.8
3.10–2.98	22,848	1,858	1,942	12.3	95.7	24.9	96.5
2.98–2.87	23,139	1,921	2,078	12.0	92.4	30.3	95.3
2.87–2.77	22,948	1,979	2,173	11.6	91.1	36.5	94.9
2.77–2.68	8,852	1,978	2,256	4.5	87.7	27.4	91.5
2.68–2.60	8,545	2,017	2,257	4.2	89.4	29.9	90.4
2.60–2.53	8,566	2,020	2,216	4.2	91.1	34.8	86.9
2.53–2.46	7,569	1,931	2,483	3.9	77.8	40.7	84.9
Total	27,1893	28,779	31,286	9.4	92.0	10.6	94.6

B. Final model statistics

Refinement statistics	
Number of atoms	
Protein: Lipase	3,490
Colipase	639
Solvent	293
Metal	1
Inhibitor	30
β-Octylglucoside	140
Resolution range (Å)	6.0–2.46
Number of reflections	27,738
R-factor ($I/\sigma I > 1$)[b]/free R-factor[c]	18.3/25.8
RMS deviation from standard geometries	
Bonds (Å)	0.013
Angles (°)	1.960
Dihedrals (°)	25.70
Impropers (°)	1.67

Average temperature factor (Å) // occupation factor	
Main-chain atoms	30.5 // 1
Side-chain atoms	34.2 // 1
Solvent atoms	44.72 // 1
Metal atoms	25.02 // 1
Inhibitor atoms	
Conformation no. 1	21.9 // 0.65
Conformation no. 2	19.82 // 0.4
β-Octylglucoside	
Molecule no. 1	26.3 // 0.5
Molecule no. 2	57.5 // 0.5
Molecule no. 3	38.5 // 0.5
Molecule no. 4	58.3 // 0.5
Molecule no. 5	58.9 // 0.5
Molecule no. 6	52.1 // 0.5
Molecule no. 7	70.0 // 0.5

[a] $R_{sym} = \Sigma_{hkl}\Sigma_{ref}|I_{hkl} - \langle I_{hkl}\rangle| / \Sigma_{hkl}\Sigma_{ref}\langle I_{hkl}\rangle$.

[b] R-factor $= \Sigma_{hkl}|F_o - F_c| / \Sigma_{hkl}|F_o|$.

[c] Brünger (1992).

The first round of refinement using reflections between 8.00 and 2.46 Å brought the R-factor from 43.7% to 24.8%. Two maps ($2F_o - F_c$ and $F_o - F_c$) computed between 20.0 and 2.46 Å resolution revealed a continuous electron density starting at the active site serine (Ser 152). The R enantiomer of the phosphonate inhibitor was fitted in the electron density map. Region 246–251 of lipase and 72–80 of colipase were reconstructed and water molecules were added when visible throughout the refinement procedure. Several cycles of S.A. refinement leave a strong residual density near Ser 152. We constructed the S enantiomer of the inhibitor in this density and refined both enantiomers with partial occupancies (0.65 and 0.40, respectively). Five detergent molecules were constructed in residual electron density of Fourier difference maps calculated between 6.00 and 2.46 Å resolution. Two of these β-octylglucoside molecules have a well-defined electron density map after refinement performed with the energy minimization of X-PLOR, whereas the third one lacks density for the glucose ring, and the two last molecules are worst defined. We attempted to refine them further using alternate conformations with the glucose ring in a common position and two different orientations for the alkyl chains. All these detergent molecules have been refined with an occupancy of 50%.

The final model includes 5,080 protein atoms, 1 calcium ion, 293 water molecules, 1 covalent inhibitor (partial occupancies, 2 enantiomers), and 5 detergent molecules (partial occupancies, 2 with alternate conformations). The final *R*-factor is 18.3% in the 6.0–2.46-Å-resolution range. The free *R*-factor is 25.8%.

B-factor statistics, bond and angle deviations from ideality were calculated with X-PLOR (Brünger et al., 1987). The Ramachandran plot was obtained with the Procheck program (Laskowski et al., 1993). Secondary structure analysis and accessible surface calculations were carried out with DSSP (Kabsch & Sander, 1983).

Acknowledgments

This work was supported by the EC BRIDGE-Lipase project (contract BIOT CT91-0274), the CNRS-IMABIO Programme, and the PACA region.

References

Alder A, Lazarus RL, Dennis MS, Wagner G. 1991. Solution structure of kristin, a potent platelet aggregation inhibitor and GP IIb-IIIa antagonist. *Science 253*:445–448.

Borgström B, Erlanson-Albertsson C. 1984. In: Borgström B, Brockman HL, eds. *Lipases*. Amsterdam: Elsevier. pp 151–183.

Borgström B, Wieloch T, Erlanson-Albertsson C. 1979. Evidence for a pancreatic pro-colipase and its activation by trypsin. *FEBS Lett 108*:407–410.

Brünger AT, Karplus M. 1991. Molecular dynamics simulations with experimental restraints. *Acc Chem Res 24*:54–61.

Brünger AT, Kuriyan J, Karplus M. 1987. Crystallographic *R* factor refinement by molecular dynamics. *Science 235*:458–460.

Canioni P, Julien R, Rathelot J, Sarda L. 1977. Inhibition of sheep pancreatic lipase activity against emulsified tributyrin by non-ionic detergents. *Lipids 12*:393–397.

Chaillan C, Kerfelec B, Foglizzo E, Chapus C. 1992. Direct involvement of the C-terminal extremity of pancreatic lipase (403–449) in colipase binding. *Biochem Biophys Res Commun 184*:206–211.

Cozzone P, Canioni P, Sarda L, Kaptein R. 1981. 360-MHz nuclear magnetic resonance and laser photochemically induced dynamic nuclear polarization studies of bile salt interaction with porcine colipase A. *Eur J Biochem 114*:119–126.

De Caro A, Figarella C, Amic J, Michel R, Guy O. 1977. Human pancreatic lipase: A glycoprotein. *Biochim Biophys Acta 490*:411–419.

Desnuelle P. 1986. Pancreatic lipase and phospholipase. In: Desnuelle P, Sjostrom H, Noren O, eds. *Molecular and cellular basis of digestion*. New York: Elsevier Science Publishing Co., Inc. pp 289–296.

Egloff MP. 1995. Études cristallographiques du système lipase pancreatique humaine-colipase, et d'une protéine de transport d'acides gras [thesis]. Orsay, France: Université de Paris-sud.

Egloff MP, Marguet F, Buono G, Verger R, Cambillau C, van Tilbeurgh H. 1995. The 2.46 Å resolution structure of the pancreatic lipase colipase complex inhibited by a C11 alkyl phosphonate. *Biochemistry*. Forthcoming.

Engh RA, Huber R. 1991. Accurate bond and angle parameters for X-ray protein-structure refinement. *Acta Crystallogr A 47*:392–401.

Erlanson C, Charles M, Astier M, Desnuelle P. 1974. The primary structure of porcine colipase II. The disulfide bridges. *Biochim Biophys Acta 359*:198–203.

Erlanson-Albertsson C. 1981. The existence of pro-colipase in pancreatic juice. *Biochim Biophys Acta 666*:299–300.

Erlanson-Albertsson C. 1992. Pancreatic colipase. Structural and physiological aspects. *Biochim Biophys Acta 1125*:1–7.

Erlanson-Albertsson C, Larsson A. 1981. Importance of the N-terminal sequence in porcine pancreatic colipase. *Biochim Biophys Acta 665*:250–255.

Erlanson-Albertsson C, Larsson A. 1988. A possible physiological function of pancreatic pro-colipase activation peptide in appetite regulation. *Biochimie 70*:1245–1250.

Erlanson-Albertsson C, Mei J, Okada S, York D, Bray GA. 1991. Pancreatic procolipase propeptide, enterostatin specially inhibits fat intake. *Physiol & Behav 49*:1185–1189.

Fukoa SI, Taniguchi Y, Kitigawa Y, Scheele G. 1990. Full length cDNA sequence encoding canine pancreatic colipase. *Nucleic Acids Res 18*:5549.

Fukoa SI, Zhang DE, Taniguchi Y, Scheele G. 1993. Structure of the canine pancreatic colipase gene includes two protein-binding sites in the protomer region. *J Biol Chem 268*:11312–11320.

Grasberger BL, Clore GM, Gronenborn AM. 1994. High-resolution structure of *Ascaris* trypsin inhibitor in solution: direct evidence for a pH-induced conformational transition in the reactive site. *Structure 2*:669–678.

Huang KH, Strynadka NCJ, Bernard VD, Peanasky RJ, James MNG. 1994. The molecular structure of the complex of chymotrypsin/elastase inhibitor with porcine elastase. *Structure 2*:679–689.

Janin J, Chothia C. 1990. The structure of protein–protein recognition sites. *J Biol Chem 265*:16027–16030.

Kabsch W, Sander C. 1983. Dictionary of protein secondary structure: Pattern recognition of hydrogen-bonded and geometrical features. *Biopolymers 22*:2577–2637.

Laskowski R, MacArthur M, Moss D, Thornton J. 1993. Procheck: A program to check the stereochemical quality of protein structures. *J Appl Crystallogr 26*:91–97.

McIntyre JC, Hundley P, Behnke WD. 1987. The role of aromatic side chain residues in micell binding by pancreatic colipase. *Biochem J 245*:821–829.

McIntyre JC, Schroeder F, Behnke WD. 1990. Synthesis and characterization of the dansyltyrosine derivatives of porcine pancreatic colipase. *Biochemistry 29*:2092–2101.

Rathelot J, Canioni P, Bosc-Bierne I, Sarda L, Kamoun A, Kaptein R, Cozzone P. 1988. Limited proteolysis of porcine and equine colipases spectroscopic and kinetics studies. *Biochim Biophys Acta 671*:155–163.

Rathelot J, Julien R, Bosc-Bierne I, Gargouri Y, Canioni P, Sarda L. 1981. Horse pancreatic lipase. Interaction with colipase from various species. *Biochimie 63*:227–234.

Renaud W, Dagorn JC. 1991. cDNA sequence and deduced amino-acid sequence of human preprocolipase. *Pancreas 6*:157–161.

Roussel A, Cambillau C. 1991. The TURBO-FRODO graphics package. In: *Silicon Graphics Directory*. Mountain View, California: Silicon Graphics.

Rugani N. 1993. Structure et fonction de la colipase pancreatique [thesis]. St-Charles, France: Université d'Aix-Marseille I, Faculté.

Rydel TJ, Tulinsky M, Bode W, Huber R. 1991. Refined structure of the hirudin–thrombin complex. *J Mol Biol 221*:583–601.

Saudek V, Atkinson A, Pelton JT. 1991. Three-dimensional structure of echistatin, the smallest active RGD protein. *Biochemistry 30*:7369–7372.

Sternby B, Borgström B. 1981. Comparative studies on the ability of pancreatic colipases to restore activity of lipases from different species. *Comp Biochem Physiol 68B*:15–18.

Sternby B, Erlanson-Albertsson C. 1982. Measurement of the binding of human colipase to human lipase and lipase substrates. *Biochim Biophys Acta 711*:193–195.

van Tilbeurgh H, Egloff MP, Martinez C, Rugani N, Verger R, Cambillau C. 1993a. Interfacial activation of the pancreatic lipase–colipase complex by mixed micelles revealed by X-ray crystallography. *Nature 362*: 814–820.

van Tilbeurgh H, Gargouri Y, Dezan C, Egloff MP, Nésa MP, Rugani N, Sarda L, Verger R, Cambillau C. 1993b. Crystallization of pancreatic procolipase and of its complex with pancreatic lipase. *J Mol Biol 229*: 552–554.

van Tilbeurgh H, Sarda L, Verger R, Cambillau C. 1992. Structure of the pancreatic lipase–procolipase comlex. *Nature 359*:159–162.